

Targeted Epithelial Tight Junction Dysfunction Causes Immune Activation and Contributes to Development of Experimental Colitis

LIPING SU,* LE SHEN,* DANIEL R. CLAYBURGH,* SAM C. NALLE,* ERIKA A. SULLIVAN,* JON B. MEDDINGS,[‡] CLARA ABRAHAM,[§] and JERROLD R. TURNER*

*Department of Pathology, The University of Chicago, Chicago, Illinois; [‡]Department of Medicine, University of Alberta, Edmonton, AB, Canada; and [§]Section of Digestive Diseases, Department of Medicine, Yale University, New Haven, Connecticut

Background & Aims: Inflammatory bowel disease (IBD) is a multifactorial disease thought to be caused by alterations in epithelial function, innate and adaptive immunity, and luminal microbiota. The specific role of epithelial barrier function remains undefined, although increased activity of intestinal epithelial myosin light chain kinase (MLCK), which is the primary mechanism of tumor necrosis factor-induced barrier dysfunction, occurs in human IBD. Our aim was to determine whether, in an intact epithelium, primary dysregulation of the intestinal epithelial barrier by pathophysiologically relevant mechanisms can contribute to development of colitis. **Methods:** We developed transgenic (Tg) mice that express constitutively active MLCK (CA-MLCK) specifically within intestinal epithelia. Their physiology, immune status, and susceptibility to disease were assessed and compared with non-Tg littermate controls. **Results:** CA-MLCK Tg mice demonstrated significant barrier loss but grew and gained weight normally and did not develop spontaneous disease. CA-MLCK Tg mice did, however, develop mucosal immune activation demonstrated by increased numbers of lamina propria CD4⁺ lymphocytes, redistribution of CD11c⁺ cells, increased production of interferon- γ and tumor necrosis factor, as well as increased expression of epithelial major histocompatibility complex class I. When challenged with CD4⁺CD45⁺Rb^{hi} lymphocytes, Tg mice developed an accelerated and more severe form of colitis and had shorter survival times than non-Tg littermates. **Conclusions:** Primary pathophysiologically relevant intestinal epithelial barrier dysfunction is insufficient to cause experimental intestinal disease but can broadly activate mucosal immune responses and accelerate the onset and severity of immune-mediated colitis.

Increased intestinal permeability, or barrier dysfunction, was recognized in patients with Crohn's disease (CD) over 25 years ago.¹ The presence of barrier dysfunction in a subset of first-degree relatives of CD patients has caused some to suggest that barrier dysfunction may contribute to disease.²⁻⁵ Given that permeability increases in CD relatives and patients with quiescent dis-

ease are limited to small molecules,^{2,4} are generally less than 2-fold,^{2-4,6} and are undetectable in some studies,⁷ there has been considerable controversy regarding their significance in CD patients and relatives. Moreover, because permeability defects can be induced by inflammation,⁸ the debate as to whether barrier dysfunction is a cause or effect of disease continues.^{4,9}

Data from experimental models, such as the interleukin (IL)-10^{-/-} mouse, demonstrate that primary immune defects can cause barrier loss that precedes overt disease.¹⁰ As a clinical correlate, CD patients with quiescent disease and increased intestinal permeability relapse at greater rates than quiescent CD patients without increased permeability.^{11,12} Thus, barrier loss may occur secondary to clinically inapparent immune dysfunction and precede active disease in CD patients and experimental models of IBD. However, no studies have examined disease risk in healthy CD relatives with increased permeability compared to healthy relatives without increased permeability. Therefore, the role of increased intestinal permeability to small molecules in CD pathogenesis remains controversial.

A landmark study of mosaic mice expressing dominant negative N-cadherin showed that intestinal epithelial dysfunction can cause experimental inflammatory bowel disease (IBD).¹³ Although barrier function was not measured in this model, it was almost certainly perturbed because dominant negative N-cadherin expression disrupted cell-cell and cell-matrix contacts as well as enterocyte differentiation and polarization.^{13,14} The conclusion that gross epithelial dysfunction can cause intestinal disease is also supported by the DSS model of colitis, in which severe mucosal damage occurs prior to the onset of inflammation,¹⁵ as well as trinitrobenzene sulfonic acid-induced colitis, which requires gross epithelial disruption by ethanol.¹⁶ Thus, barrier disruption in many disease models is secondary to severe damage that includes areas

Abbreviations used in this paper: CA-MLCK, constitutively active myosin light chain kinase; MLC, myosin II regulatory light chain; MLCK, myosin light chain kinase; PIK, membrane Permeant Inhibitor of myosin light chain Kinase; Tg, transgenic; WT, wild-type.

© 2009 by the AGA Institute

0016-5085/09/\$36.00

doi:10.1053/j.gastro.2008.10.081

of ulceration with nearly complete epithelial loss. Such barrier loss is quantitatively massive and very different from the defined changes in paracellular permeability that occur in CD patients and, more critically, their healthy first-degree relatives. Thus, the barrier defects induced by global epithelial dysfunction or damage do not address the significance of increased paracellular permeability in CD patients and their relatives.

The principal determinant of paracellular permeability in an intact epithelium is the intercellular tight junction. Unfortunately, no available experimental models target intestinal epithelial tight junction barrier function without disrupting other critical cellular functions. This deficit has limited our understanding of the role of barrier dysfunction in disease initiation and perpetuation. The 2 primary pathways of tight junction regulation described in IBD involve acute changes mediated by the cytoskeleton and more chronic changes induced by modifications in claudin protein expression.¹⁷ Both mechanisms can be triggered by cytokines. Tumor necrosis factor (TNF)-induced barrier loss is primarily due to myosin II regulatory light chain (MLC) phosphorylation by myosin light chain kinase (MLCK), both in vitro and in vivo.^{18,19} The presence of increased MLC phosphorylation in IBD patients²⁰ indicates that this mechanism is relevant to human disease.

To assess the role of barrier dysfunction in disease initiation and perpetuation, we developed a transgenic (Tg) mouse expressing constitutively active MLCK (CA-MLCK) within intestinal epithelia. This CA-MLCK expression triggers MLC phosphorylation and increases intestinal epithelial tight junction permeability. The increased permeability is qualitatively and quantitatively similar to that observed in healthy relatives of CD patients, and, therefore, these mice represent a targeted model to assess the effects of tight junction barrier dysfunction on intestinal disease. CA-MLCK Tg animals are clinically normal. However, the barrier defects induced by epithelial CA-MLCK expression trigger increased production of proinflammatory and immunoregulatory cytokines, expansion of lamina propria CD4⁺ T cells, and redistribution of CD11c⁺ cells within the intestinal mucosa. Moreover, adoptive transfer colitis develops more rapidly, and disease severity is increased in CA-MLCK Tg mice. These data, therefore, show that primary tight junction dysfunction can trigger subclinical mucosal immune activation. Moreover, these events enhance disease progression when combined with a second, nonepithelial defect, emphasizing the critical interplay between the epithelium and immune system in maintaining intestinal homeostasis.

Materials and Methods

Generation of CA-MLCK Tg mice

The constitutively active MLCK construct²¹ was ligated into the p3xFLAG CMV10 vector (Sigma, St Louis, MO) to place 3X FLAG at the N-terminus and

introduced into a vector containing the intestinal epithelial cell-specific 9-kilobase villin promoter.²² Tg and wild-type (WT) mice were maintained in a specific pathogen-free facility and studied with Institutional Animal Care and Use Committee approval.

Immunofluorescence

Frozen sections were fixed in 1% paraformaldehyde, blocked, and incubated with antibodies against FLAG, phosphorylated MLC, BrdU, Ki-67, CD4, Gr-1, CD68, CD11c, junctional adhesion molecule-A (JAM-A), claudin-1, occludin, ZO-1 (Abcam, Cambridge, MA; AbD Serotec, Raleigh, NC; BD Biosciences, San Jose, CA; eBioscience, San Diego, CA; Invitrogen, Carlsbad, CA; Neomarkers, Fremont, CA) followed by appropriate Alexa dye-conjugated secondary immune reagents, Alexa dye-conjugated phalloidin, and Hoechst 33342 (Invitrogen).¹⁸ Mice were injected intraperitoneally with 25 mg/kg BrdU and killed at indicated times after injection. Sections were incubated for 15 minutes with 2 N HCl prior to immunostaining. For morphometry, at least 10–15 fields or crypts from ≥ 3 mice were examined.

Intestinal Permeability

Jejunal permeability was determined as previously described.¹⁸ Colonic permeability was assessed as sucralose and creatinine fractional recovery over 16 hours following gavage with 15 mg creatinine and 9 mg sucralose.^{23,24}

Flow Cytometry

Intraepithelial lymphocytes and lamina propria lymphocytes were isolated and stained as described.²⁵ Recovered cells were evaluated using a BD FACSCalibur (BD Biosciences). Data were normalized to the mean values for WT mice.

Quantitative Polymerase Chain Reaction

Minced proximal colon was sonicated in TRIzol and RNA extracted with chloroform, precipitated, and further purified using an RNeasy mini kit (Qiagen, Valencia, CA). Complementary DNA was synthesized with reverse transcriptase (Invitrogen), and messenger RNA (mRNA) was quantified by SYBR green real-time polymerase chain reaction (PCR) (Bio-Rad, Hercules, CA) using validated primers.

Serum Endotoxin Assay and Microbiologic Culture

Serum endotoxin was measured by limulus amoebocyte lysate assay (Associates of Cape Cod, East Falmouth, MA) and was >4 U/mL in septic mice. Blood was cultured aerobically on Brucella agar (BD Biosciences). Spleen and mesenteric lymph node homogenates were plated and cultured aerobically on brain-heart infusion and MacConkey agar and anaerobically on Brucella agar. Numerous colonies were identified on all plates from septic controls.

CD4⁺CD45Rb^{hi} Colitis Model

CD4⁺CD45Rb^{hi} and CD4⁺CD45Rb^{lo} splenocytes were isolated using a MoFlo Cell Sorter (Beckman Coulter, Fullerton, CA), and 500,000 cells were injected intravenously into 6-week-old mice. Sections of proximal colon were processed routinely; stained by H&E; and scored semiquantitatively from 0 to 3 each for lymphoid infiltrates, polymorphonuclear infiltrates, transmural inflammation, mucosal hyperplasia, epithelial mucin depletion, epithelial apoptosis, erosions, and crypt architectural distortion. Interferon (IFN)- γ and TNF protein were assessed in tissue lysates by enzyme-linked immunosorbent assay (eBioscience).

Statistical Analysis

All data are presented as mean \pm SE. All experiments were performed with triplicate or greater samples, and data shown are representative of 3 or more independent studies. *P* value was determined by Student *t* test, Fisher exact test, or the log-rank test (survival) and considered significant if less than .05.

Results

To develop a model system in which intestinal tight junction permeability was increased via a targeted, pathophysiologically relevant mechanism, we established Tg mice expressing a CA-MLCK expressed under control of the 9-kilobase villin promoter (Figure 1A). CA-MLCK was expressed strongly in small intestine and colon but

was only detected faintly in kidney (Figure 1B). No CA-MLCK expression was detected in brain, lung, heart, or liver (Figure 1B). Immunofluorescence microscopy confirmed that intestinal CA-MLCK expression was exclusively epithelial (Figure 1C). CA-MLCK expression in the kidney was below the level of detection by immunofluorescence microscopy (data not shown).

CA-MLCK Causes Intestinal Epithelial MLC Phosphorylation and Barrier Regulation

In vitro CA-MLCK expression is sufficient for regulation of tight junction barrier function.²¹ CA-MLCK Tg mice are far more complex, and compensatory changes to prevent or correct MLC phosphorylation induced by CA-MLCK may occur. We therefore assessed MLC phosphorylation spatially and quantitatively. MLC phosphorylation was increased, primarily within the perijunctional actomyosin ring, of jejunal and colonic epithelia in CA-MLCK Tg mice (Figure 2A). Quantitative analysis showed 76% and 51% increases in MLC phosphorylation in isolated jejunal and colonic epithelia, respectively (Figure 2B and C; *P* < .01). These increases are comparable to those observed following expression of CA-MLCK in cultured monolayers²¹ and to previously reported in vitro and in vivo increases in MLC phosphorylation associated with barrier regulation.^{18,26} To verify that the increased MLC phosphorylation was due to MLCK enzymatic activity, jejunal and colonic segments were perfused with the specific MLCK inhibitor PIK (membrane Permeant Inhibitor of myosin light chain Kinase).¹⁹ This completely reversed Tg-induced increases in MLC phosphorylation (Figure 2B and C; *P* < .05). Thus, increased MLC phosphorylation observed in jejunal and colonic epithelia of CA-MLCK Tg mice is the result of CA-MLCK enzymatic activity and not secondary compensatory changes.

To assess the effects of CA-MLCK Tg expression on jejunal paracellular permeability, an established in vivo perfusion system was used.¹⁸ CA-MLCK Tg mice demonstrated a 65% increase in paracellular flux, corresponding to a 0.11 $\mu\text{g}/\text{cm}/\text{h}$ increase in albumin efflux (Figure 2D; *P* < .01), similar to the 0.17 $\mu\text{g}/\text{cm}/\text{h}$ increase induced by intraperitoneal injection of 5 μg TNF.²⁷ Inclusion of PIK in the jejunal perfusion solution completely corrected the barrier defect in CA-MLCK mice (Figure 2D; *P* < .01), demonstrating that CA-MLCK enzymatic activity is the direct cause of increased paracellular permeability.

Technical limitations preclude analysis of colonic paracellular permeability by in vivo perfusion. Instead, fractional urinary recovery of sucralose and creatinine was assessed in a manner similar to the assay used in CD patients and relatives. Creatinine and sucralose recovery in CA-MLCK Tg mice was 154% and 170% of WT mice, respectively (Figure 2E; *P* < .02). These are comparable to the 139% increase in PEG-400 recovery reported in CD patients.² Thus, CA-MLCK expression causes increases in small intestinal and colonic para-

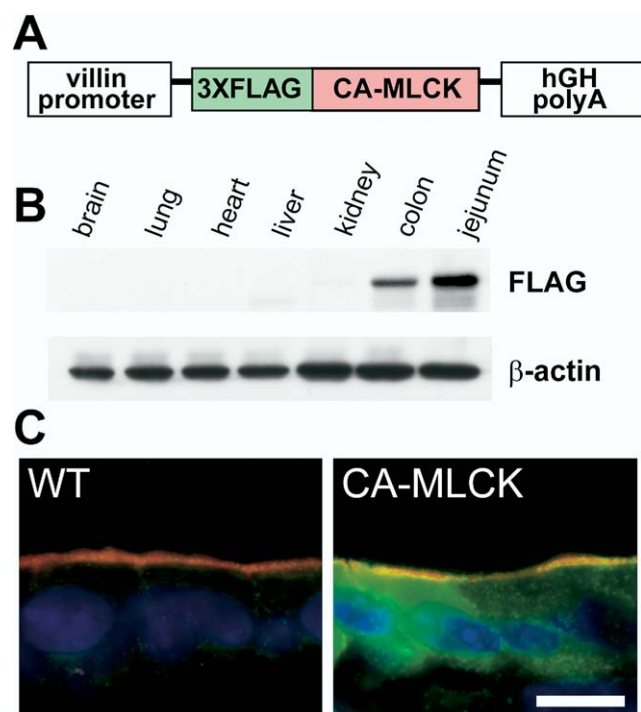


Figure 1. Generation of CA-MLCK mice. (A) The CA-MLCK transgene construct. (B) Immunoblot of indicated organs from CA-MLCK Tg mice. (C) CA-MLCK, detected via the FLAG epitope tag (green), in jejunal epithelium. F-actin (red) and nuclei (blue) are shown. Bar, 10 μm .

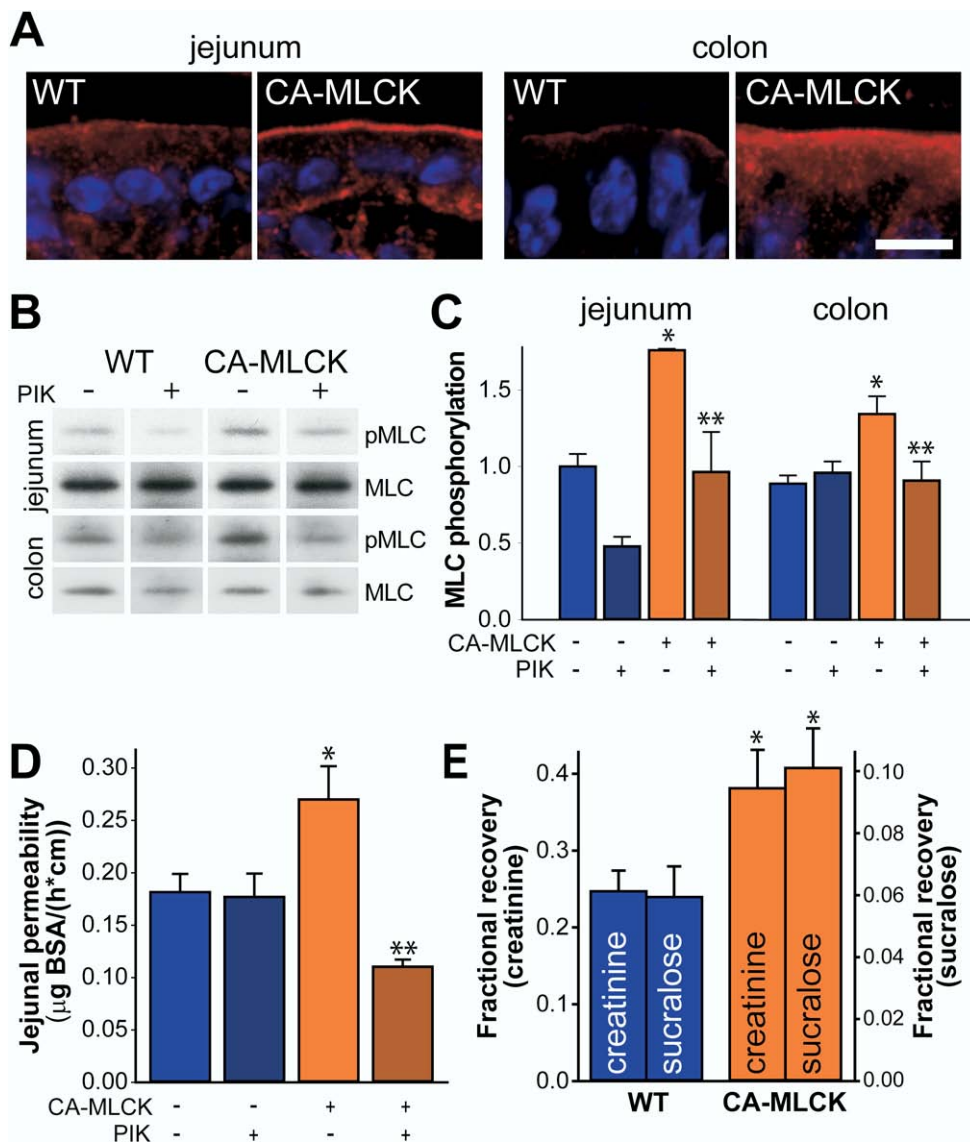


Figure 2. CA-MLCK expression causes intestinal epithelial MLC phosphorylation and intestinal barrier dysfunction. (A) Phosphorylated MLC (red) in jejunum and colon of WT and CA-MLCK Tg mice. Nuclei are shown in blue. Bar, 10 μm . (B and C) Immunoblot of phosphorylated MLC (pMLC) and total MLC and densitometric analysis of samples from WT (blue bars) and CA-MLCK Tg (orange bars) mice after in vivo perfusion with (dark bars) or without (light bars) PIK, $n = 4$ for each condition. * $P < .01$ vs WT littermates; ** $P < .05$ vs CA-MLCK Tg mice without PIK. (D) Paracellular BSA flux with or without PIK, $n = 4$ for each condition. * $P < .01$ vs WT; ** $P < .01$ vs Tg without PIK. (E) In vivo measurement of colonic paracellular permeability in WT and CA-MLCK Tg mice. * $P < .02$ vs WT.

cellular permeability that are quantitatively and qualitatively similar to those present in CD patients and their relatives.

Tight Junction Morphology Is Intact in CA-MLCK Tg Mice

We have previously reported that CA-MLCK expression in cell monolayers causes only mild alterations of tight junction structure.²¹ To assess this in vivo, we examined the distributions of claudin-1, occludin, ZO-1, and JAM-A in CA-MLCK Tg mice (Figure 3). The localization of these tight junction proteins in both crypt and surface epithelium of CA-MLCK Tg mice was similar to that in WT littermates.

Chronically Increased Paracellular Permeability Is Insufficient to Cause Disease

CA-MLCK Tg pups were born in the expected Mendelian proportions, grew and gained weight identically to gender-matched littermates (Figure 4A), and were

without histopathologic disease as late as 52 weeks of age (Figure 4B). To exclude accelerated epithelial turnover, Ki-67 expression was assessed and found to be limited to the crypt and transit-amplifying cell populations (Figure 4C and D). BrdU incorporation was used to independently assess epithelial proliferation and migration, and there was no difference between CA-MLCK Tg and WT mice (Figure 4E and F). Thus, CA-MLCK Tg mice are free of symptomatic or histologic intestinal disease. These mice present a unique opportunity to study the impact of pathophysiologically relevant barrier dysfunction on mucosal homeostasis.

Increased Paracellular Permeability Alters Lamina Propria Immune Status

To assess the activation status of the mucosal immune system, intraepithelial and lamina propria lymphocytes were isolated from WT and CA-MLCK Tg mice. Small increases in the fraction of CD69⁺ and CD62L^{lo}

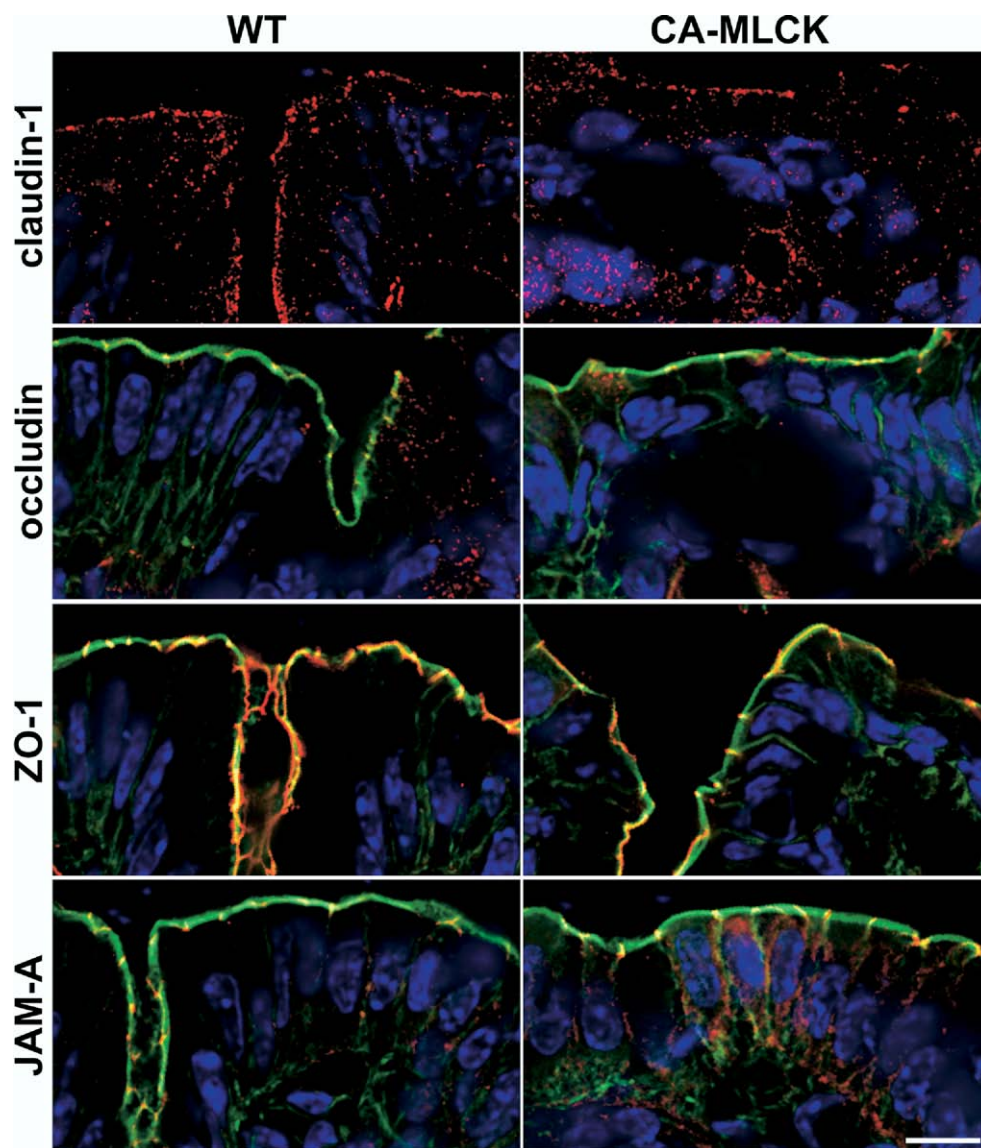


Figure 3. CA-MLCK Tg mice do not display alterations in tight junction organization. Immunostains of tight junction-associated proteins in colonic mucosa of CA-MLCK Tg and WT mice. Junctional proteins (claudin-1, occludin, ZO-1, JAM-A) are shown in red. Nuclei are blue. F-actin is shown in green in the images of occludin, ZO-1, and JAM-A. Bar, 10 μ m.

expressing cells were present among CD4⁺ intraepithelial lymphocytes and CD8⁺ lamina propria lymphocytes, respectively, from CA-MLCK Tg mice (Figure 5A and B; $P < .02$). Although statistically significant, these changes are small and were only present in the minority T-cell population in each compartment. Thus, we sought to better assess absolute numbers of mucosal lymphocytes. A 40% increase in numbers of lamina propria CD4⁺ lymphocytes was present in CA-MLCK Tg mice (Figure 5C; $P < .03$), suggesting mucosal immune cell recruitment or proliferation secondary to barrier dysfunction.

Further characterization of CA-MLCK Tg mice demonstrated a mild increase in numbers of mucosal neutrophils, assessed by Gr-1 immunostaining, although this was not statistically significant (Figure 5D; $P > .1$). There were also no differences in total numbers of mucosal macrophages, detected by CD68 expression (Figure 5E) or dendritic cells, assessed as CD11c⁺ cells (Figure 5F).

However, there was a striking redistribution of CD11c⁺ cells to the superficial lamina propria of CA-MLCK Tg mice. Only 26% of mucosal CD11c⁺ cells were present in the luminal half of the lamina propria in WT mice, whereas 58% of CD11c⁺ cells were present in the superficial half of the lamina propria in CA-MLCK Tg mice (Figure 4F; $P < .01$). Although macrophages can express CD11c, the lack of change in the number and distribution of CD68⁺ macrophages suggests that the differentially distributed CD11c⁺ cells are dendritic cells. Thus, epithelial CA-MLCK expression triggers mild mucosal immune activation.

Subclinical Mucosal Immune Activation Is Present in CA-MLCK Tg Mice

To further characterize mucosal immune activation induced by CA-MLCK expression, cytokine expression was assessed. At 3 weeks of age, mucosal production of IFN- γ , TNF, IL-4, IL-5, IL-10, IL-17, IL-23, and trans-

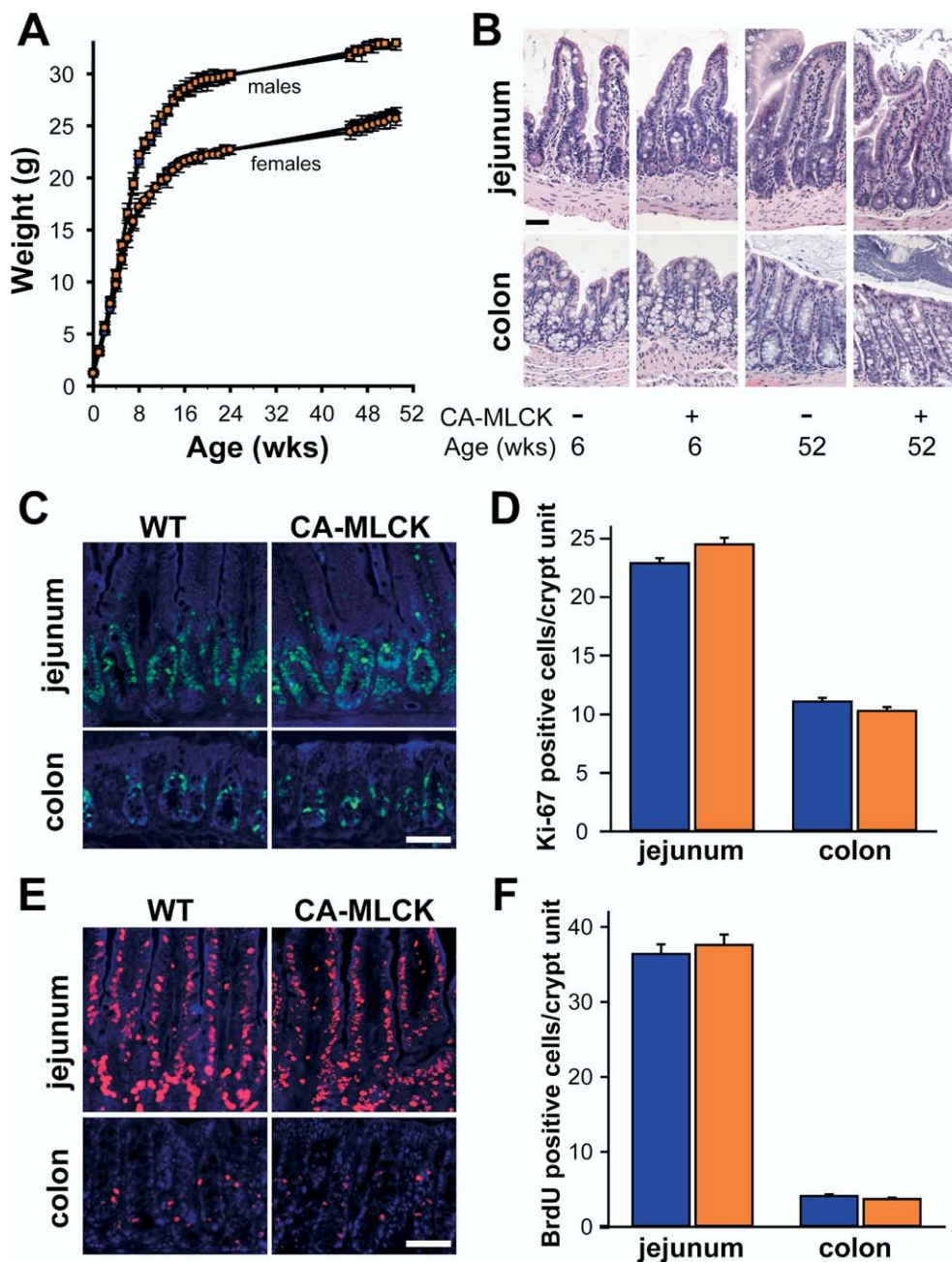


Figure 4. CA-MLCK Tg mice grow normally and do not display histologic disease. (A) Growth of CA-MLCK Tg (orange symbols) and WT (blue symbols) mice (male, squares; female, circles). (B) Jejunum and proximal colon of CA-MLCK Tg and WT mice at 6 and 52 weeks of age, respectively. Bar, 50 μ m. (C and D) Ki-67 (green) in jejunum and proximal colon of CA-MLCK Tg (orange bars) and WT (blue bars) mice. Bar, 30 μ m. (E and F) BrdU (red) incorporation and morphometry of CA-MLCK Tg (orange bars) and WT (blue bars) mice in jejunum and proximal colon epithelium after 36 hours and 2 hours, respectively. Bar, 30 μ m.

forming growth factor (TGF)- β transcripts was identical in Tg and littermate control mice (Figure 6A). By 6 weeks of age, all mice displayed increases in mucosal transcripts for IFN- γ , TNF, IL-10, and TGF- β relative to the levels measured at 3 weeks of age ($P < .05$). Whereas TGF- β transcript increases were similar in CA-MLCK Tg mice and WT littermates, IFN- γ , TNF, and IL-10 transcripts were significantly greater in 6-week-old CA-MLCK Tg mice than WT littermates ($P < .03$). These differences persisted at 52 weeks of age. Increased numbers of lamina propria CD4 $^{+}$ T lymphocytes in CA-MLCK Tg mice could not explain increased cytokine transcripts because the 40% increase in CD4 $^{+}$ lymphocytes is far less than the 2.6- to 13.6-fold increases in transcripts. Moreover, dif-

ferences in transcript expression remained significant when normalized to CD3 or CD4 transcripts rather than GAPDH.

Elevated mucosal IFN- γ and TNF transcription suggests T helper cell (Th)1 polarization, whereas the absence of IL-17 or IL-23 increases suggests that Th17 expansion did not occur in CA-MLCK Tg mice. To assess Th1/Th2 balance, the transcription factors T-bet and GATA-3, which drive CD4 $^{+}$ T lymphocytes toward Th1 or Th2 differentiation pathways, respectively, were measured. The T-bet/GATA-3 ratio of CA-MLCK Tg mice was similar to littermate controls at 3 weeks of age (Figure 6B). However, the T-bet/GATA-3 ratio of CA-MLCK Tg mice nearly doubled by 6 weeks and similarly remained

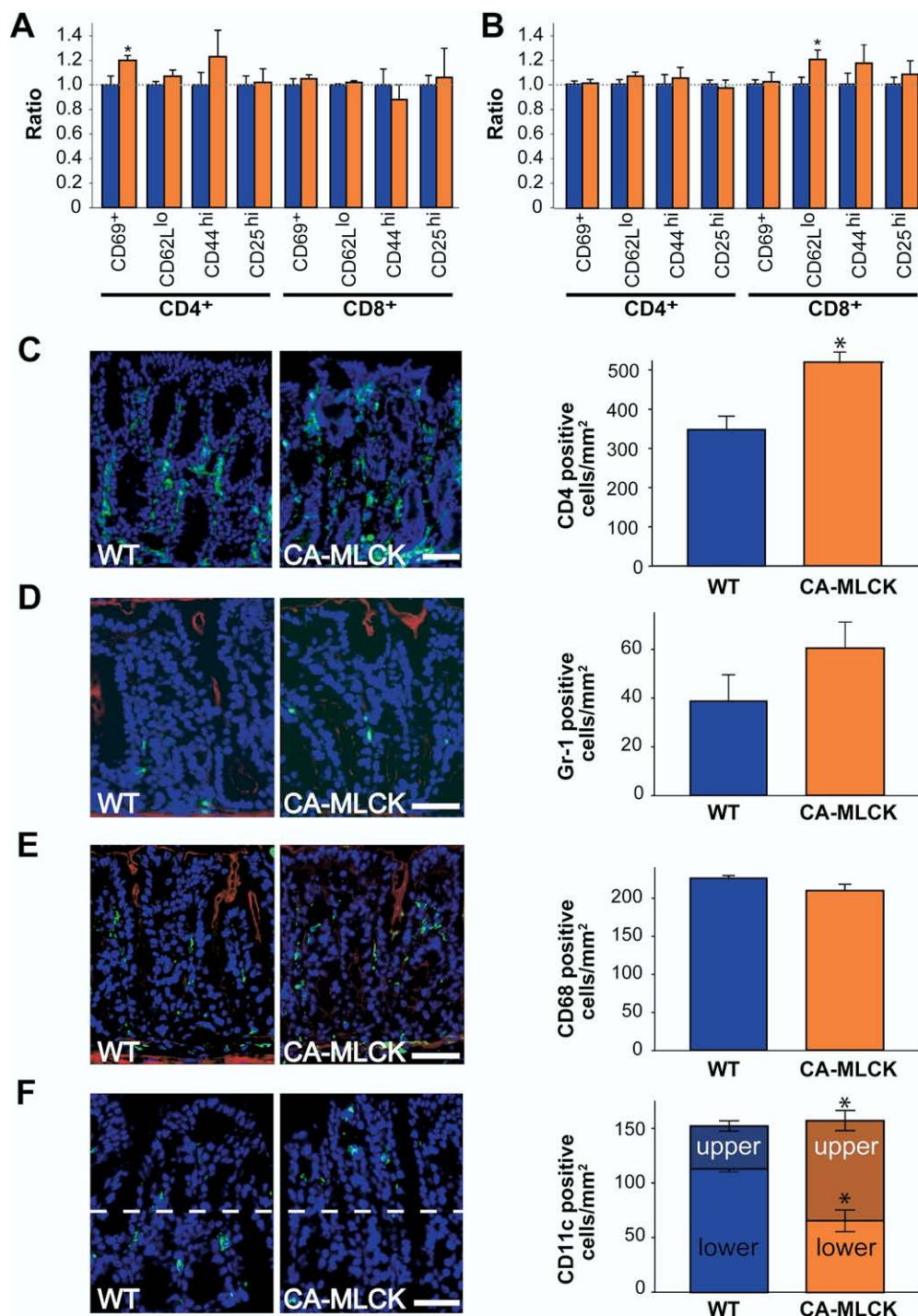


Figure 5. Increased paracellular permeability modifies lamina propria immune cell recruitment. (A) Intraepithelial lymphocytes of WT (blue bars) and CA-MLCK Tg (orange bars) mice. $*P < .02$ vs WT. (B) Lamina propria lymphocytes were harvested from colon of WT (blue bars) and CA-MLCK Tg (orange bars) mice. $*P < .02$ vs WT. (C) CD4⁺ cells (green) in the colonic lamina propria of WT and CA-MLCK Tg mice. Morphometric analysis of WT (blue bar) and CA-MLCK Tg (orange bar) mice is shown. Bar, 50 μ m. $*P < .03$. (D) Gr-1⁺ cells (green) in the colonic lamina propria of WT and CA-MLCK Tg mice. F-actin is shown in red. Morphometric analysis is shown. Bar, 50 μ m. (E) CD68⁺ cells (green) in the colonic lamina propria of WT and CA-MLCK Tg mice. F-actin is shown in red. Morphometric analysis is shown. Bar, 50 μ m. (F) CD11c⁺ cells (green) in the colonic lamina propria of WT and CA-MLCK Tg mice. F-actin is shown in red. Morphometric analysis is shown at right, separating superficial (dark shading) and basal (light shading) sections of the lamina propria. Bar, 40 μ m. $*P < .01$.

elevated at 52 weeks of age ($P < .02$), consistent with lifelong Th1 polarization. We therefore asked whether Foxp3⁺ Tregs might be expanded to prevent disease in CA-MLCK Tg mice. Mucosal Foxp3 expression was not altered in response to CA-MLCK expression in 3- or 6-week-old mice, but a minor increase was present at 52 weeks (Figure 6C).

The absence of clinical or histologic disease in CA-MLCK Tg mice may reflect enhanced regulatory input, as indicated by elevated mucosal expression of IL-10 and, in older mice, Foxp3 transcripts. Alternatively, it

may simply be that epithelial CA-MLCK expression generates too small a stimulus to trigger disease, regardless of immunoregulatory responses. We therefore asked whether the observed changes were sufficient to affect epithelial expression of the class I major histocompatibility complex (MHC), which can be stimulated by a variety of cytokines including IFN- γ .²⁸ Immunoblot of isolated epithelia and immunofluorescence microscopy demonstrated increased epithelial H-2Kb expression within both surface and crypt epithelium of CA-MLCK Tg mice (Figure 6D). Thus,

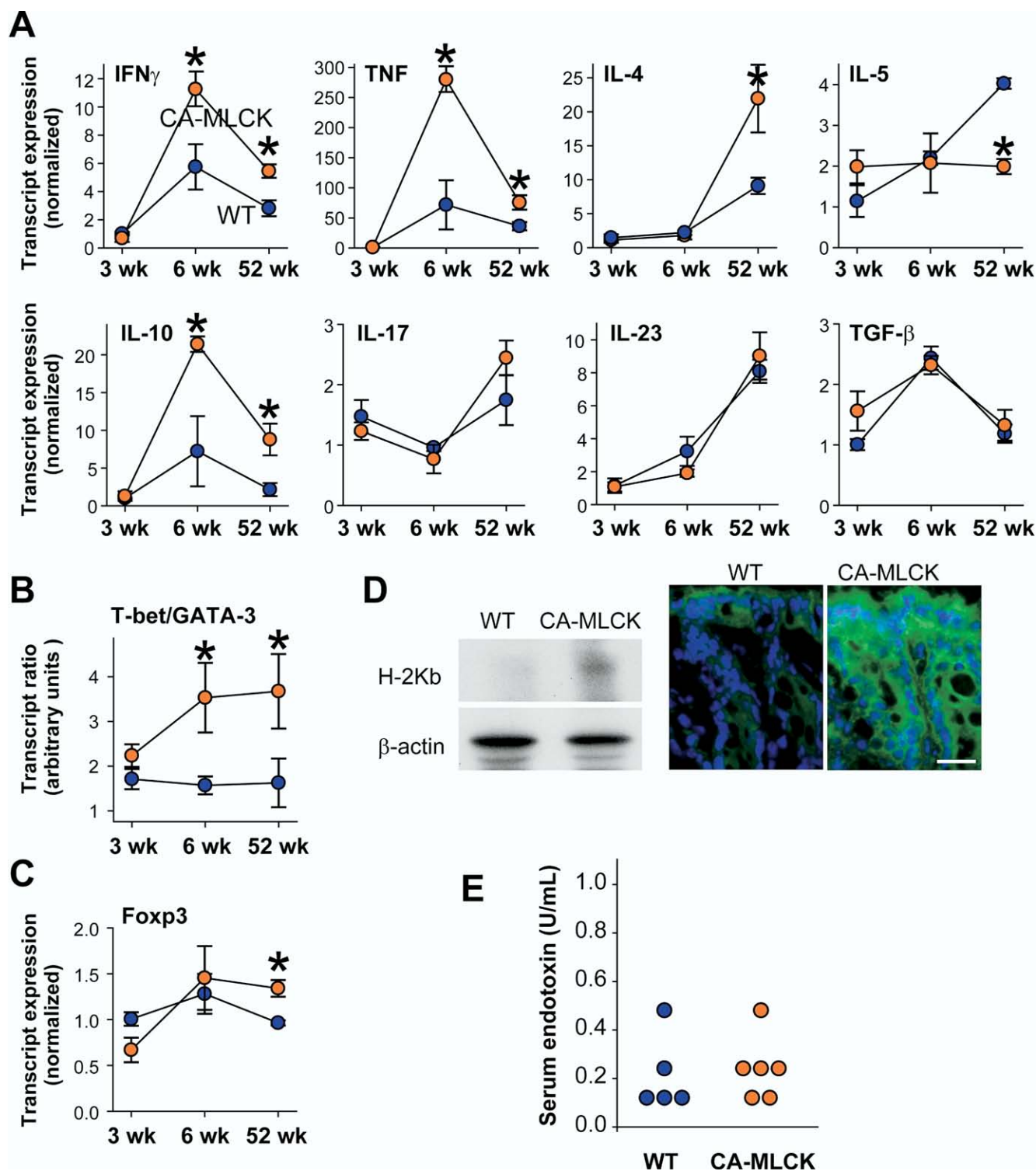


Figure 6. Subclinical mucosal immune activation is present in CA-MLCK Tg mice. (A) Transcript content for indicated cytokines in proximal colon of WT (blue symbols) and CA-MLCK Tg (orange symbols) mice. * $P < .03$. (B) T-bet/GATA-3 transcript ratios in WT (blue symbols) and CA-MLCK Tg (orange symbols) mice at 3 weeks, 6 weeks, and 52 weeks of age. * $P < .02$. (C) Foxp3 transcript expression in WT and Tg * $P < .02$. (D) H2Kb expression was assessed by SDS-PAGE and immunoblot in isolated colonic epithelial cells of WT and CA-MLCK mice. Immunofluorescence detection of H2Kb expression (green) in colonic epithelium of WT and CA-MLCK mice. Bar, 20 μ m. (E) Endotoxin assay showed similar quantities in serum of WT (blue symbols) and CA-MLCK Tg (orange symbols) mice.

CD4⁺ lymphocyte expansion, altered trafficking of CD11c⁺ cells, Th1 polarization, and epithelial MHC expression all support the conclusion that subclinical mucosal immune activation is present in CA-MLCK Tg

mice. This is, therefore, the first demonstration of a targeted, pathophysiologically relevant disturbance of epithelial tight junction barrier function leading to immune activation.

CA-MLCK-Induced Increases in Paracellular Permeability Do Not Result in Transfer of Bacteria or Endotoxin to Serum or Secondary Lymphoid Organs

To determine whether increased bacterial translocation could explain the mucosal immune activation observed in CA-MLCK Tg mice, we assayed serum endotoxin and cultured mesenteric lymph nodes, spleen, and blood. Serum endotoxin was detectable in all mice but was not different between CA-MLCK Tg mice and WT littermates (Figure 6E; $P > .2$). No growth was observed in most cases, and the number of samples from which colonies grew was similar when CA-MLCK Tg and WT littermates were compared ($n = 7$; $P > .2$). Thus, neither increased systemic circulation of microbial products nor increased bacterial translocation into secondary lymphoid organs are present in CA-MLCK Tg mice.

Paracellular Barrier Defects Accelerate Onset and Enhance Severity of Colitis

CA-MLCK Tg mice provide a unique opportunity to assess the relevance of increased paracellular permeability to disease development. The data above show that, despite mild mucosal immune activation, disease does not develop in CA-MLCK Tg mice housed under specific pathogen-free conditions. However, it may be that the CA-MLCK Tg mice are more susceptible to illness should an appropriate stimulus be provided. This is consistent with current understanding of human IBD, which likely also involves perturbations of multiple, separate processes.

To address disease susceptibility in CA-MLCK Tg mice, we sought a pathophysiologically relevant colitis model that is not initiated by massive epithelial injury. We selected the well-established $CD4^+CD45Rb^{hi}$ adoptive transfer model of colitis, which has many similarities to human IBD, including roles for IFN- γ and TNF.²⁹ This model is ideal because (1) disease can be limited by transfer of Tregs,³⁰ (2) disease is abrogated in the absence of MyD88-dependent bacterial signaling,³¹ and (3) epithelial disruption is not required to cause disease.²⁹

The $CD4^+CD45Rb^{hi}$ adoptive transfer model requires immunodeficient recipients. RAG1 $^{-/-}$ mice expressing the CA-MLCK Tg were bred and showed similar CA-MLCK expression to immunocompetent Tg mice. Moreover, mucosal IFN- γ , TNF, and IL-10 transcripts were elevated in 6-week-old CA-MLCK Tg, RAG1 $^{-/-}$ mice, relative to RAG1 $^{-/-}$ littermates (Figure 7A; $P < .01$), indicating that the increased cytokine transcription observed is, at least partially, derived from innate immune cells.

Six-week-old CA-MLCK Tg, RAG1 $^{-/-}$ mice and RAG1 $^{-/-}$ littermates were adoptively transferred with $CD4^+CD45Rb^{hi}$ T lymphocytes from WT mice. $CD4^+CD45Rb^{lo}$ T lymphocytes, given as a control, did not cause weight loss or other clinical evidence of disease (Figure 7B). RAG1 $^{-/-}$ mice receiving $CD4^+CD45Rb^{hi}$ T lymphocytes fell below their starting weight 19 days after

adoptive transfer. CA-MLCK Tg, RAG1 $^{-/-}$ mice began to lose weight much earlier and fell below their initial weights after 12 days. Thus, disease onset was significantly earlier in CA-MLCK Tg mice (Figure 7B; $P < .05$).

Consistent with earlier clinical presentation in CA-MLCK Tg recipients, mucosal expression of IFN- γ and TNF transcripts ($P < .03$) and protein ($P < .04$) was markedly increased at early times after adoptive transfer (Figure 7C). Even at later times, when all mice were clinically ill and weight loss in Tg and non-Tg mice was similar, expression of IFN- γ and TNF transcripts and protein remained significantly greater in CA-MLCK Tg mice (Figure 7C).

Histopathology of disease was qualitatively similar in CA-MLCK Tg mice and littermate controls and was characterized by lymphoid and polymorphonuclear infiltrates, transmural inflammation, mucosal hyperplasia, epithelial mucin depletion and apoptosis, erosions, and crypt architectural distortion. However, severity of damage was far greater in CA-MLCK Tg mice. This was true both at early times after adoptive transfer (Figure 7D and E; $P < .01$) and at later times as disease progressed ($P < .03$). Thus, when taken together, the increased cytokine production and more severe mucosal disease induced in the presence of intestinal epithelial CA-MLCK Tg expression suggest that overall disease is worsened by pathophysiologically relevant tight junction barrier dysfunction.

To further investigate disease severity, survival after $CD4^+CD45Rb^{hi}$ T lymphocyte adoptive transfer was assessed. Only 55% of CA-MLCK Tg mice were alive 42 days after adoptive transfer and 20% remained alive at 84 days (Figure 7F). In contrast, 88% of littermates were alive 42 days after adoptive transfer, and 55% were alive after 84 days ($P < .05$). Thus, in addition to significantly earlier disease onset, increased IFN- γ and TNF expression, and more severe histopathology, survival of CA-MLCK Tg mice after $CD4^+CD45Rb^{hi}$ lymphocyte transfer was significantly worse than that of their littermates. These data therefore show that targeted, epithelial-specific CA-MLCK Tg expression accelerates disease onset, increases severity, and hastens mortality due to colitis. Moreover, because the trigger for this colitis was adoptive transfer of naïve T cells, these data show, for the first time, that pathophysiologically relevant epithelial barrier dysfunction, in the absence of gross epithelial damage, can synergize with immune defects to enhance disease pathogenesis.

Discussion

Increased intestinal permeability in CD patients and some of their healthy relatives suggests that barrier defects may be an inciting factor in CD.²⁻⁴ This idea is consistent with the hypothesis that barrier defects result in antigen leakage, mucosal immune activation, and clinical disease. However, immune dysregulation can also cause barrier loss, supporting the alternative hypothesis

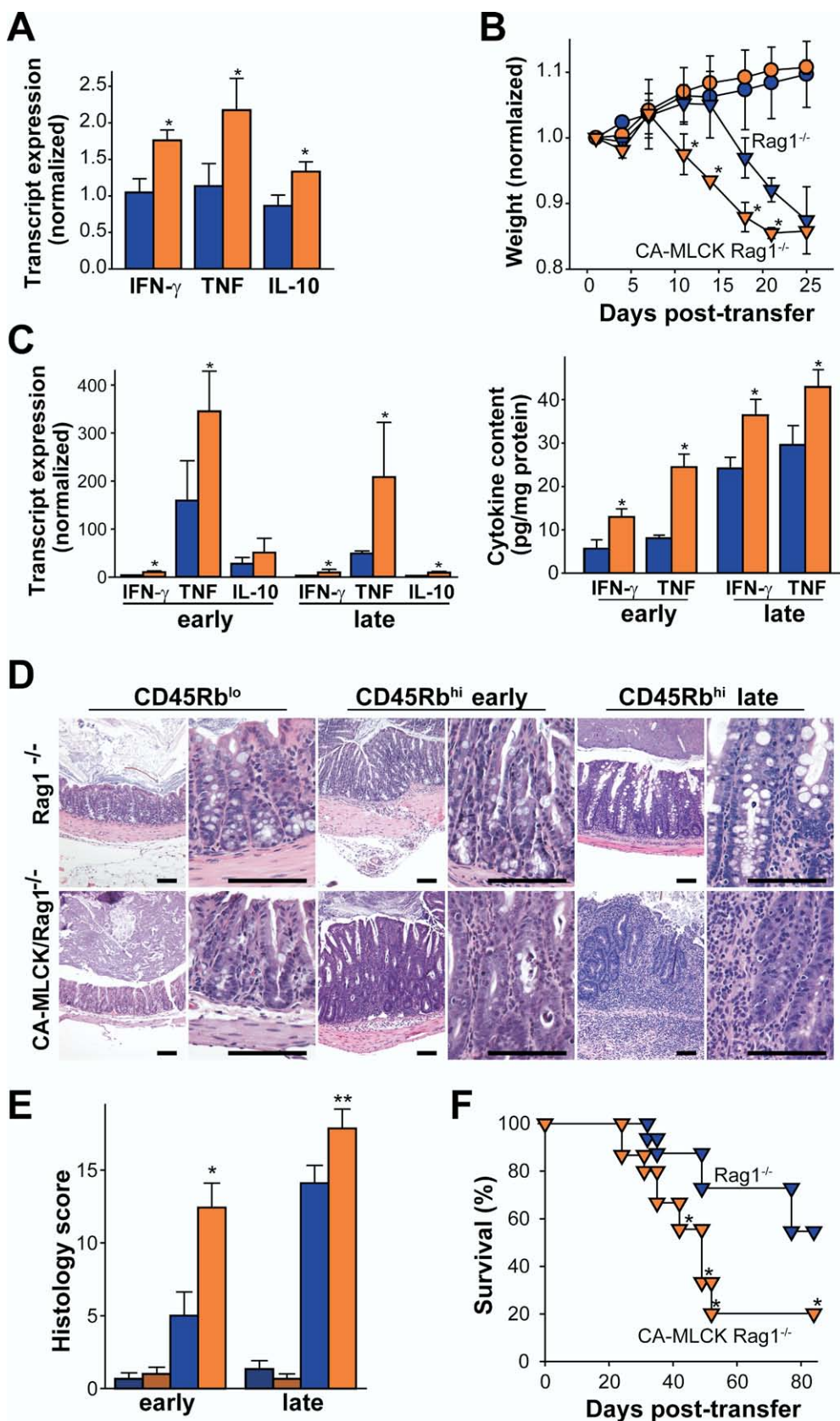


Figure 7. Increased paracellular permeability accelerates immune-mediated colitis. (A) Transcript content in proximal colon of 6-week-old RAG1^{-/-} (blue bars) and CA-MLCK Tg, RAG1^{-/-} (orange bars) mice, prior to adoptive transfer. **P* < .01. (B) Weight after adoptive transfer of CD4⁺CD45Rb^{hi} (triangles) and CD4⁺CD45Rb^{lo} (circles) T cells into RAG1^{-/-} (blue symbols) and CA-MLCK Tg, RAG1^{-/-} (orange symbols) recipients. Weights were normalized to weight prior to adoptive transfer. **P* < .05 vs RAG1^{-/-} recipients receiving CD4⁺CD45Rb^{hi} T cells. (C) Transcript content in proximal colon of RAG1^{-/-} (blue bars) and CA-MLCK Tg, RAG1^{-/-} (orange bars) mice 12 days (early) or 19 days (late) after adoptive transfer. **P* < .03. Changes in IFN- γ and TNF protein expression were similar. **P* < .04 (D) Colon histology 12 days (early) and 19 days (late) after adoptive transfer. Bar, 100 μ m. (E) Histology scores of the proximal colon sections of RAG1^{-/-} (blue bars) and CA-MLCK Tg, RAG1^{-/-} (orange bars) mice 12 days (early) and 19 days (late) after adoptive transfer. **P* < .01 vs RAG1^{-/-} recipients transferred with CD4⁺CD45Rb^{hi} T cells, ***P* < .03 vs RAG1^{-/-} recipients transferred with CD4⁺CD45Rb^{lo} T cells. (F) Survival of RAG1^{-/-} (blue symbols) and CA-MLCK Tg, RAG1^{-/-} (orange symbols) recipients after transfer of CD4⁺CD45Rb^{hi} T cells. **P* < .05.

that observed permeability defects are secondary to immune signaling. We sought to differentiate between primary barrier defects and those secondary to immune activation by directly targeting the intestinal epithelium. We altered tight junction permeability via MLCK activation because (1) tight junction dysregulation is well documented in IBD,^{17,32} (2) MLCK activation is present in intestinal epithelia of IBD patients,²⁰ (3) MLCK activation is required for in vivo TNF-induced tight junction dysregulation,¹⁸ and (4) MLCK activation is sufficient to regulate tight junctions in vitro.²¹ CA-MLCK Tg mice demonstrated increased MLC phosphorylation and barrier defects similar to those in CD patients and a subset of their healthy first-degree relatives.²⁻⁴ Moreover, mild immune activation is present in CA-MLCK Tg mice. Thus, these data show that epithelial tight junction dysregulation similar to that seen in healthy CD relatives with barrier defects can cause subclinical mucosal immune activation.

Both the design of the CA-MLCK Tg mouse and the results obtained differentiate this from existing models of disease in which barrier dysfunction has been observed in association with defects that extend beyond the tight junction.^{13-16,33-36} For example, although systemic knockout of JAM-A does not result in spontaneous disease, DSS induces colitis of enhanced severity in these mice,³⁶ consistent with the contributions of JAM-A to epithelial and endothelial barrier function and inflammatory cell migration.³⁶ Although mucosal immune status of JAM-A^{-/-} mice has not been examined, this would be of interest given our data showing that targeted expression of CA-MLCK in intestinal epithelia does cause mucosal immune activation.

No longitudinal studies correlating risk of developing disease with intestinal permeability in healthy relatives of CD patients have been reported. Thus, the hypothesis that increased intestinal permeability is a risk factor for disease development is untested. Even if barrier defects are assumed to be an initiating event in CD, increased permeability may be present many years before the onset of CD in human subjects.³⁷ Thus, 1 or more additional predisposing factors are likely present. The identity of these factors is unknown, but they are likely to include immune dysregulation and altered luminal microbiota. CA-MLCK Tg mice provide a targeted, pathophysiologically relevant model of tight junction dysregulation for direct analysis of the role of primary increases in paracellular permeability in intestinal disease. We employed the well-characterized CD4⁺CD45Rb^{hi} adoptive transfer model of immune-mediated colitis,²⁹ which has many similarities to human IBD and targets a pathway distinct from epithelial barrier regulation, in lieu of the currently unidentified factors that trigger disease onset in human patients. Onset of weight loss was earlier in CA-MLCK Tg mice, mucosal cytokine expression was greater, histopathology was more severe, and survival was poorer. Thus, although insufficient to initiate disease, these data show

that targeted, pathophysiologically relevant intestinal epithelial tight junction dysregulation can amplify the cycle of inflammation and accelerate progression of immune-mediated colitis.

The question remains, how does barrier dysfunction increase susceptibility to experimental disease? Our analyses of healthy CA-MLCK Tg mice suggest that chronically increased paracellular permeability is sufficient to cause mucosal immune activation. This is amply demonstrated by the mild increases in IFN- γ and TNF transcription and increased T-bet/GATA-3 ratio detected as well as cellular changes, such as increased mucosal CD4⁺ lymphocytes and enhanced epithelial MHC class I expression. The data indicate that this mucosal immune activation is associated with Th1 polarization. Although the significance of CD11c⁺ cell redistribution toward the lumen is not clear, it is interesting to note that enrichment of dendritic cells at the superficial mucosa has been observed during the early stages of *Campylobacter* colitis in human patients³⁸ and that dendritic cell redistribution has also been associated with nonsteroidal anti-inflammatory drug-induced colitis in rats.³⁹

One might also ask why CA-MLCK Tg mice are not ill. Although this will require further analysis, it may be that increased mucosal IL-10 and, in elderly mice, Foxp3⁺ transcript expression reflects immunoregulatory mechanisms that prevent disease. This is consistent with a recent report showing that transient epithelial damage activates immunoregulatory responses.⁴⁰

It has long been hypothesized that barrier dysfunction contributes to the development of colitis secondary to increased translocation of luminal bacteria. To assess this, we asked whether serum endotoxin was elevated in CA-MLCK Tg mice; it was not. Similarly, microbiologic culture of blood and secondary lymphoid organs demonstrated no difference between CA-MLCK Tg mice and WT littermates. Thus, the systemic load of bacteria and bacterial products was not increased in CA-MLCK Tg mice. However, these data do not exclude a role for increased paracellular flux of luminal bacterial products in CA-MLCK Tg mice. Rather, they suggest that the effect of increased tight junction permeability may be to allow local increases in flux of bacterial products. Thus, it will be important to assess immune activation in antibiotic-treated and germ-free CA-MLCK Tg mice, as well as those colonized with defined microbes, in the future. Data from such studies will help to determine the potential impact of limited and local mucosal immune responses on systemic disease.

In conclusion, these data are the first to demonstrate that targeted, pathophysiologically relevant regulation of intestinal epithelial tight junctions induces mucosal immune activation. The novel and mechanistically accurate model provided by the CA-MLCK Tg mice also represents the only experimental model to recapitulate the observation in humans that isolated increases in paracellular permeability are insufficient to cause disease. Finally,

these data demonstrate that increases in intestinal epithelial paracellular permeability can predispose and contribute to pathogenesis and progression of experimental colitis and suggest that the same may be true in human IBD.

References

- Pearson AD, Eastham EJ, Laker MF, et al. Intestinal permeability in children with Crohn's disease and coeliac disease. *Br Med J (Clin Res Ed)* 1982;285:20–21.
- Hollander D, Vadheim CM, Brettholz E, et al. Increased intestinal permeability in patients with Crohn's disease and their relatives. A possible etiologic factor. *Ann Intern Med* 1986;105:883–885.
- May GR, Sutherland LR, Meddings JB. Is small intestinal permeability really increased in relatives of patients with Crohn's disease? *Gastroenterology* 1993;104:1627–1632.
- Katz KD, Hollander D, Vadheim CM, et al. Intestinal permeability in patients with Crohn's disease and their healthy relatives. *Gastroenterology* 1989;97:927–931.
- Clayburgh DR, Shen L, Turner JR. A porous defense: the leaky epithelial barrier in intestinal disease. *Lab Invest* 2004;84:282–291.
- Soderholm JD, Peterson KH, Olaison G, et al. Epithelial permeability to proteins in the noninflamed ileum of Crohn's disease? *Gastroenterology* 1999;117:65–72.
- Teahon K, Smethurst P, Levi AJ, et al. Intestinal permeability in patients with Crohn's disease and their first degree relatives. *Gut* 1992;33:320–323.
- Miki K, Moore DJ, Butler RN, et al. The sugar permeability test reflects disease activity in children and adolescents with inflammatory bowel disease. *J Pediatr* 1998;133:750–754.
- Sartor RB. Microbial influences in inflammatory bowel diseases. *Gastroenterology* 2008;134:577–594.
- Madsen KL, Malfair D, Gray D, et al. Interleukin-10 gene-deficient mice develop a primary intestinal permeability defect in response to enteric microflora. *Inflamm Bowel Dis* 1999;5:262–270.
- D'Inca R, Di Leo V, Corrao G, et al. Intestinal permeability test as a predictor of clinical course in Crohn's disease. *Am J Gastroenterol* 1999;94:2956–2960.
- Wyatt J, Vogelsang H, Hubl W, et al. Intestinal permeability and the prediction of relapse in Crohn's disease. *Lancet* 1993;341:1437–1439.
- Hermiston ML, Gordon JI. Inflammatory bowel disease and adenomas in mice expressing a dominant negative N-cadherin. *Science* 1995;270:1203–1207.
- Hermiston ML, Gordon JI. In vivo analysis of cadherin function in the mouse intestinal epithelium: essential roles in adhesion, maintenance of differentiation, and regulation of programmed cell death. *J Cell Biol* 1995;129:489–506.
- Cooper HS, Murthy SN, Shah RS, et al. Clinicopathologic study of dextran sulfate sodium experimental murine colitis. *Lab Invest* 1993;69:238–249.
- Yamada Y, Marshall S, Specian RD, et al. A comparative analysis of two models of colitis in rats. *Gastroenterology* 1992;102:1524–1534.
- Weber CR, Turner JR. Inflammatory bowel disease: is it really just another break in the wall? *Gut* 2007;56:6–8.
- Clayburgh DR, Barrett TA, Tang Y, et al. Epithelial myosin light chain kinase-dependent barrier dysfunction mediates T cell activation-induced diarrhea in vivo. *J Clin Invest* 2005;115:2702–2715.
- Zolotarevsky Y, Hecht G, Koutsouris A, et al. A membrane-permeant peptide that inhibits MLC kinase restores barrier function in vitro models of intestinal disease. *Gastroenterology* 2002;123:163–172.
- Blair SA, Kane SV, Clayburgh DR, et al. Epithelial myosin light chain kinase expression and activity are up-regulated in inflammatory bowel disease. *Lab Invest* 2006;86:191–201.
- Shen L, Black ED, Witkowski ED, et al. Myosin light chain phosphorylation regulates barrier function by remodeling tight junction structure. *J Cell Sci* 2006;119:2095–2106.
- Pinto D, Robine S, Jaisser F, et al. Regulatory sequences of the mouse villin gene that efficiently drive transgenic expression in immature and differentiated epithelial cells of small and large intestines. *J Biol Chem* 1999;274:6476–6482.
- Meddings JB, Gibbons I. Discrimination of site-specific alterations in gastrointestinal permeability in the rat. *Gastroenterology* 1998;114:83–92.
- Turner JR, Cohen DE, Mrsny RJ, et al. Noninvasive in vivo analysis of human small intestinal paracellular absorption: regulation by Na⁺-glucose cotransport. *Dig Dis Sci* 2000;45:2122–2126.
- Marski M, Kandula S, Turner JR, et al. CD18 is required for optimal development and function of CD4+CD25+ T regulatory cells. *J Immunol* 2005;175:7889–7897.
- Turner JR, Rill BK, Carlson SL, et al. Physiological regulation of epithelial tight junctions is associated with myosin light-chain phosphorylation. *Am J Physiol* 1997;273:C1378–C1385.
- Clayburgh DR, Musch MW, Leitges M, et al. Coordinated epithelial NHE3 inhibition and barrier dysfunction are required for TNF-mediated diarrhea in vivo. *J Clin Invest* 2006;116:2682–2694.
- Colgan SP, Parkos CA, Matthews JB, et al. Interferon- γ induces a cell surface phenotype switch on T84 intestinal epithelial cells. *Am J Physiol* 1994;267:C402–C410.
- Powrie F, Leach MW, Mauze S, et al. Inhibition of Th1 responses prevents inflammatory bowel disease in scid mice reconstituted with CD45RBhi CD4+ T cells. *Immunity* 1994;1:553–562.
- Mottet C, Uhlig HH, Powrie F. Cutting edge: cure of colitis by CD4+CD25+ regulatory T cells. *J Immunol* 2003;170:3939–3943.
- Fukata M, Breglio K, Chen A, et al. The myeloid differentiation factor 88 (MyD88) is required for CD4+ T-cell effector function in a murine model of inflammatory bowel disease. *J Immunol* 2008;180:1886–1894.
- Zeissig S, Burgel N, Gunzel D, et al. Changes in expression and distribution of claudin 2, 5 and 8 lead to discontinuous tight junctions and barrier dysfunction in active Crohn's disease. *Gut* 2007;56:61–72.
- Olson TS, Reuter BK, Scott KG, et al. The primary defect in experimental ileitis originates from a nonhematopoietic source. *J Exp Med* 2006;203:541–552.
- Collett A, Higgs NB, Gironella M, et al. Early molecular and functional changes in colonic epithelium that precede increased gut permeability during colitis development in *mdr1a*(–/–) mice. *Inflamm Bowel Dis* 2008;14:620–631.
- Resta-Lenert S, Smitham J, Barrett KE. Epithelial dysfunction associated with the development of colitis in conventionally housed *mdr1a* –/– mice. *Am J Physiol Gastrointest Liver Physiol* 2005;289:G153–G162.
- Vetrano S, Rescigno M, Rosaria Cera M, et al. Unique role of junctional adhesion molecule-a in maintaining mucosal homeostasis in inflammatory bowel disease. *Gastroenterology* 2008;135:173–184.
- Irvine EJ, Marshall JK. Increased intestinal permeability precedes the onset of Crohn's disease in a subject with familial risk. *Gastroenterology* 2000;119:1740–1744.
- Pulimood AB, Ramakrishna BS, Rita AB, et al. Early activation of mucosal dendritic cells and macrophages in acute *Campylobacter colitis* and cholera: an in vivo study. *J Gastroenterol Hepatol* 2008;23:752–758.
- Silva MA, Porras M, Jury J, et al. Characterization of ileal dendritic cell distribution in a rat model of acute and chronic inflammation. *Inflamm Bowel Dis* 2006;12:457–470.

40. Boirivant M, Amendola A, Butera A, et al. A transient breach in the epithelial barrier leads to regulatory T-cell generation and resistance to experimental colitis. *Gastroenterology* 2008;135:1612–1623.e5.

Received August 18, 2008. Accepted October 30, 2008.

Address correspondence to: Jerrold R. Turner, MD, PhD, Department of Pathology, The University of Chicago, 5841 South Maryland, MC 1089, Chicago, Illinois 60637. e-mail: jturner@bsd.uchicago.edu or Clara Abraham, MD, Section of Digestive Diseases, Yale University, 333 Cedar Street, LMP 1080, New Haven, CT 06520. clara.abraham@yale.edu.

Supported by the NIH (grants R01DK61931, R01DK68271, R01DK77905, and P01DK67887), the Crohn's and Colitis Foundation of America, the University of Chicago Cancer Center (P30CA14599), a research fellowship award from the Crohn's and Colitis Foundation of America sponsored by Laura McAteer Hoffman (to L. Shen), and by T32GM07281 and T32HL007237 (to D.R.C., S.C.N., and E.A.S.).

The authors thank L. Degenstein for outstanding technical assistance, Y.-X. Fu for insightful discussion, V. Guerriero for providing a CA-MLCK template, S. Robine and D. Louvard for providing the villin promotor, C.R. Weber for statistical assistance, and L. Zitzow for critical advice.

C. Abraham and J.R. Turner contributed equally to this paper.

The authors disclose no conflicts.